

DESY 83-094
LAPP-TH 88
September 1983



MESON AND BARYON MASSES FOR LIGHT KOGUT-SUSSKIND

QUARKS ON A LARGE LATTICE

by

J.P. Gilchrist and H. Schneider

Deutsches Elektronen-Synchrotron DESY, Hamburg

G. Schierholz

II. Institut für Theoretische Physik, Universität Hamburg

M. Teper

L.A.P.P., Annecy

ISSN 0418-9833

NOTKESTRASSE 85 · 2 HAMBURG 52

DESY behält sich alle Rechte für den Fall der Schutzrechtserteilung und für die wirtschaftliche Verwertung der in diesem Bericht enthaltenen Informationen vor.

DESY reserves all rights for commercial use of information included in this report, especially in case of apply for or grant of patents.

To be sure that your preprints are promptly included in the
HIGH ENERGY PHYSICS INDEX ,
send them to the following address (if possible by air mail) :

DESY
Bibliothek
Notkestrasse 85
2 Hamburg 52
Germany

Meson and Baryon Masses for Light Kogut-Susskind
Quarks on a Large Lattice

J.P. Gilchrist and H. Schneider
Deutsches Elektronen-Synchrotron DESY, Hamburg

G. Schierholz

II. Institut für Theoretische Physik der Universität Hamburg

M. Teper
L.A.P.P., Annecy

Abstract

We calculate meson and baryon masses in quenched QCD for the small quark masses of phenomenological interest on a $10^3 \cdot 16$ lattice. We use Kogut-Susskind fermions which possess an explicit continuous chiral symmetry. We verify that this chiral symmetry is spontaneously broken and that for the physics involved our lattice is effectively of infinite volume. At the quark masses we calculate. We verify $m_{\pi}^2 \sim m_q$, which is what one expects for a Goldstone pion. For $\Lambda_{\text{mom}} = 200$ MeV, which appears to be the consistent scale of quenched QCD, we find $m_{\rho} \approx 7$ MeV and the hadron masses $m_{\rho} = (730 \pm 90)$ MeV, $m_{A_1} = (1190 \pm 90)$ MeV, $m_{\epsilon} = (660 \pm 50)$ MeV and $m_N = (920 \pm 100)$ MeV. We also extract $f_{\pi} \approx 134$ MeV. In physical units our lattice is 3 fermi across.

In this letter we present the first results of a Monte Carlo calculation of the meson and baryon spectrum in (lattice-regularized) quenched QCD. We differ from previous (Monte Carlo) spectrum calculations in several ways: we use Kogut-Susskind staggered fermions (1), which possess a continuous chiral symmetry (instead of Wilson fermions (2), which have no chiral symmetry); we calculate directly with light quark masses; we work on a $10^3 \cdot 16$ lattice, which we check to be large enough to accommodate the dynamics of spontaneous chiral symmetry breaking and the hadrons themselves.

The dynamics that most obviously influences the character of the hadron spectrum is that of chiral symmetry and its spontaneous breaking. Therefore the action one uses should explicitly possess a chiral symmetry in the range of couplings where one performs the calculation. The Wilson fermion action (2) breaks chiral symmetry by operators, which should become irrelevant deep enough into the continuum limit. However, there is no evidence that this has happened yet in the range of couplings numerically accessible at present. The fact that the promise of the early calculations (3) on very small lattices was not fulfilled by later, more detailed work (4) emphasized for us the dangers of using Wilson fermions. This was widely interpreted at the time as a problem of finite size effects (5), with the cure to be found by increasing the lattice size. That finite size effects were a part of the problem was clear. However, there was also the disturbing possibility that these effects were being magnified by the forced extrapolation of mass measurements taken at large pion masses to zero pion mass in a theory, that perhaps had not yet developed a chiral symmetry that could be spontaneously broken. Recent calculations with Wilson fermions on large $10^3 \cdot 20$ (6) and 16^4 (7) lattices have in fact shown that the problems are still there, con-

firming our suspicion that the real problems go deeper. (A recent attempt (8) to calculate $\langle \bar{\psi}\psi \rangle$ with Wilson fermions in SU(2) suggests that continuum chiral symmetry is indeed not yet restored.)

The energy scale of the gauge dynamics is $\Lambda_{\text{mom}} = O(200 \text{ MeV})$ (see below). This is therefore also the a priori energy difference that distinguishes the chirally symmetric and chirally non-symmetric vacua. It is clear therefore that if we are to be sensitive to the spontaneous chiral symmetry breaking physics, we must choose the invariant quark mass to be $m_q \ll \Lambda_{\text{mom}}$. For example it is only in this region that one expects to find a dependence $m_q^2 \sim m_q$, which reflects the Goldstone boson character of the pion. For $m_q \gtrsim \Lambda_{\text{mom}}$ no such simple relation is to be expected. Therefore we choose to calculate with invariant quark masses in the range 10 to 100 MeV (in contrast to previous calculations with Kogut-Susskind fermions which use $m_q \gtrsim \Lambda_{\text{mom}}$ and extrapolate to small m_q by hand). We use the conjugate gradient algorithm, which is the recommended algorithm for contemporary large sparse matrix inversion, and find very accurate convergence at the small m_q of interest. This algorithm is given explicitly in ref. 9, and some general references may be found in ref. 10.

We perform our calculation at $\beta = 5.7$. We judge the lattice spacing at this β to be small enough not to distort the non-perturbative glue dynamics. For example, we find that the 0^{++} and 2^{++} glueball masses show continuum scaling behaviour (11,12) for $\beta \gtrsim 5.3$, and $\beta = 5.7$ sits at a point on the far shoulder of the specific heat peak, where the non-perturbative piece of the plaquette is dominated by the $F_{\mu\nu}^a F_{\mu\nu}^a$ operator and higher order (irrelevant) operators are still small (12).

The question of spontaneous chiral symmetry breaking needs to be addressed separately. First one needs to demonstrate the presence of such a spontaneous breaking for Kogut-Susskind fermions. This has been done in ref. 9 and ref. 13. In Fig. 1 we display a figure taken from ref. 13 showing the volume dependence of the chiral condensate $\langle \bar{\psi}\psi(m_q) \rangle$ at $\beta = 5.7$. The $10^3 \cdot 16$ points are obtained from the measurements in this paper and are taken at the masses we study here. We explicitly see that, within the small errors, a $10^3 \cdot 16$ lattice at this β and for these m_q is essentially of infinite volume as far as the dynamics of spontaneous chiral symmetry breaking is concerned.

Using the best measured values of the string tension (14), the gluon condensate (12) $\langle \frac{\alpha_s}{\pi} F_{\mu\nu}^a F_{\mu\nu}^a \rangle$ and the chiral condensate (13) $\langle \bar{\psi}\psi \rangle$, which (within $\approx 1\sigma$) consistently give

$$\Lambda_{\text{mom}} \approx 200 \text{ MeV}, \tag{1}$$

one obtains an estimate for the lattice spacing

$$a(\beta = 5.7) = 1.37 \text{ GeV}^{-1} = 0.28 \text{ fermi}. \tag{2}$$

So the spatial extent of our lattice is

$$10 a(\beta = 5.7) \approx 2.8 \text{ fermi} \approx 2 D_H, \tag{3}$$

where D_H is a typical hadron (i.e. meson or baryon) diameter. This seems a reasonably generous space for the hadron on a lattice (with antiperiodic fermionic boundary conditions; see below). Later on we shall find that (the same) $\Lambda_{\text{mom}} \approx 200 \text{ MeV}$ also fits the low-lying meson and baryon masses.

The lattice QCD action may be written in terms of the gauge field and fermion

action as

$$S = S_G + S_F \quad (4)$$

For the gauge field action we assume the standard Wilson (15) form

$$S_G = \frac{\beta}{6} \sum_{n, \mu, \nu \neq \mu} \text{Tr} (U_{n, \mu} U_{n+\nu, \nu} U_{n+\nu, \mu}^{\dagger} U_{n, \nu}^{\dagger}) \quad (5)$$

with periodic boundary conditions. As has been stated we shall use Kogut-Susskind staggered fermions (1). They are identical to naive fermions if one only excites one of their four decoupled modes. The naive fermion action is

$$S_F \equiv - \bar{\psi} [M(U) + \kappa m a] \psi \quad (6)$$

$$= - \sum_{n, \mu} \bar{\psi}_n \delta_{\mu}^{\nu} [U_{n, \mu} \psi_{n+\mu} - U_{n-\mu, \mu}^{\dagger} \psi_{n-\mu}] - \kappa m a \sum_n \bar{\psi}_n \psi_n$$

If we decompose the (antihermitean) matrix M into

$$M = \Gamma \mathcal{K} \Gamma^{\dagger} \quad (7)$$

where Γ is a unitary block diagonal matrix containing all the δ^{μ} matrices (16), and write

$$\psi = \Gamma \chi \quad (8)$$

the fermion action (6) becomes

$$S_F = - \bar{\chi} [\mathcal{K}(U) + \kappa m a] \chi \quad (9)$$

where the different components of \mathcal{K} decouple. This allows us to work with a single component fermion field, say $\tilde{\chi} = \begin{pmatrix} \chi_1 \\ 0 \\ 0 \end{pmatrix}$. Replacing χ by $\tilde{\chi}$ in

equ. (9) then gives us the action for staggered fermions. The bare quark mass m translates into the renormalization group invariant quark mass m_q introduced earlier on by

$$m_q = \alpha \frac{-4}{11} m, \quad \alpha_{\text{mom}} = \frac{g_{\text{mom}}}{4\pi} \quad (10)$$

To satisfy positivity we shall use antiperiodic boundary conditions for fermions.

The action for staggered fermions represents four flavours with a full $U(4) \times U(4)$ symmetry for $m = 0$ in the naive continuum limit. At finite lattice spacing the symmetry is explicitly broken down to $U(1) \times U(1)$ by an irrelevant operator, which mixes flavours. The important point is that the continuous $U(1)$ chiral symmetry (which we have shown (9,13) in Fig. 1 to be spontaneously broken) is not the singlet $U(1)$ axial current, whose divergence is non-zero due to the topological charge density, but belongs to the axial $SU(4)$. For a more detailed discussion see ref. 17.

The rather complex flavour structure of the staggered fermions does not have to concern us (in the quenched approximation and for all quark masses equal) as long as our meson and baryon operators have a non-trivial projection onto mesons and baryons made out of the proper combination of flavours (17).

So for the pseudoscalar, vector, pseudovector, scalar and tensor mesons we use the local operators $\bar{\psi}_m \delta_5^{\mu} \psi_m$, $\bar{\psi}_m \delta_5^{\mu} \gamma_{\nu} \psi_m$, $\bar{\psi}_m \delta_5^{\mu} \delta_5^{\nu} \psi_m$, $\bar{\psi}_m \psi_m$ and $\bar{\psi}_m \gamma_{\mu\nu} \psi_m$, respectively, which project onto the π, S, A, ϵ (i.e. the $(I, J)^{PC} = (0, 0)^{++}$ singlet) and B, while for the baryons we use the local operators $\epsilon_{ABC} (\psi_m^A \psi_m^B \psi_m^C)$

and $\epsilon_{ABC} (\psi_m^A \psi_p^B \psi_n^C)$, which project onto the nucleon (N) and Δ and their negative parity partners. The quantities we then study are the resulting meson and baryon (zero momentum) propagators (16,18)

$$\begin{aligned}
 M_{PS}(n_t) &= \sum_{\vec{n}} M(\vec{n}, n_t) = C_H e^{-m_H a n_t} + \dots + (n_t \rightarrow 16 - n_t), \\
 M_{V-T}(n_t) &= \sum_{\vec{n}} [(-1)^{n_x+n_y+n_z+(-1)^{n_0}}] M(\vec{n}, n_t) = C_G e^{-m_G a n_t} + (-1)^{n_t} C_B e^{-m_B a n_t} \\
 &\quad + \dots + (n_t \rightarrow 16 - n_t), \\
 M_{PV}(n_t) &= \sum_{\vec{n}} [(-1)^{n_x+n_y+n_z+(-1)^{n_0}}] M(\vec{n}, n_t) = C_{A_1} e^{-m_{A_1} a n_t} \\
 &\quad + (-1)^{n_t} C_G e^{-m_G a n_t} + \dots + (n_t \rightarrow 16 - n_t), \\
 M_S(n_t) &= \sum_{\vec{n}} (-1)^{n_x+n_y+n_z+n_t} M(\vec{n}, n_t) = C_E e^{-m_E a n_t} + (-1)^{n_t} C_{\pi} e^{-m_{\pi} a n_t} \\
 &\quad + \dots + (n_t \rightarrow 16 - n_t), \\
 B(n_t) &= \sum_{\vec{n}, n_2, n_3 = \text{even}} B(\vec{n}, n_t) = C_N e^{-m_N a n_t} + C_{\Delta} e^{-m_{\Delta} a n_t} + \dots \\
 &\quad + (-1)^{n_t} C_{N^-} e^{-m_{N^-} a n_t} + \dots \\
 &\quad - (-1)^{n_t} (n_t \rightarrow 16 - n_t), \\
 M(\vec{n}, n_t) &= \sum_{A,B} |G^{AB}(n)|^2, \quad G^{AB}(n) = [(\mathcal{M} + 2ma)^{-1}]^{AB} \\
 B(\vec{n}, n_t) &= \sum_{A,B,C} \epsilon_{ABC} \epsilon_{A'B'C'} G^{AA'}(n) G^{BB'}(n) G^{CC'}(n), \quad (11) \\
 &\quad A'B'C'
 \end{aligned}$$

where N^- denotes the opposite parity nucleon. M_{PV} , M_S also receive contributions from ρ , π , etc., as indicated, through some mesonic operators not listed.

We calculate 112 rows ($\times 3$ colours) of $(\mathcal{M} + 2ma)^{-1}$ on 7 independent gauge field configurations. The rows are chosen so that the quark starts well away from the spatial boundaries. We perform this calculation at masses $ma = 0.01$, 0.03 and 0.05 ($m_{\pi} \approx 14, 46$ and 73 MeV). To invert the fermion matrix we use the conjugate gradient algorithm as we have already mentioned. This algorithm solves a matrix equation $\vec{A}\vec{x} = \vec{b}$ (in our case $A = \mathcal{M} + 2ma$; \vec{b} is a unit vector, so \vec{x} is an appropriate column of A^{-1}) by minimizing $r^2 = |\vec{A}\vec{x} - \vec{b}|^2$ through an iterative procedure that produces a sequence $\{\vec{x}_i\}$ of increasingly better approximations to the desired solution. We monitor the values of $r_i^2 = |\vec{A}\vec{x}_i - \vec{b}|^2$ during our calculation. We stop the iterative procedure once $r_i^2 \leq 10^{-8}$. This means the errors on our correlation functions will be dominated by statistical rather than systematic errors.

We use the measured quark propagators to obtain M_{PS} , M_{V-T} , M_{PV} , M_S and B. We fit the pion propagator M_{PS} by two masses, m_{π} and $m_{\pi'}$. The result for m_{π} is shown in Fig. 2a. We observe that the pion mass varies with the quark mass as $m_{\pi} \sim m_q$, which is what one expects for a Goldstone pion. The dashed line in Fig. 2a follows

$$(m_{\pi} a)^2 = 7.60 ma. \quad (12)$$

For $m_{\pi'}$ we find a linear mass dependence. M_{V-T} shows only a small admixture of B, which helps to determine m_{ρ} . We fit the $2 \leq n_t \leq 14$ tail of M_{V-T} by the ρ and B mass. We use this m_{ρ} in M_{PV} to obtain m_{A_1} . The pion admixture in

M_S comes out very small in spite of the small pion mass. We fit M_S for $2\sqrt{n_c} \ll 14$ by m_c and the previously obtained pion mass. The baryon propagator B shows small errors for even n_c , while for odd n_c the errors come out to be somewhat bigger. This does not allow, at present, to separate the \bar{N} and also to give a meaningful value for m_Δ . We therefore restrict ourselves to the nucleon and fit the $2\sqrt{n_c} \ll 14$ tail of B by m_N . The results for m_g , m_{A_1} , m_c and m_N are shown in Fig. 2b. The calculated hadron masses can be interpolated by the linear mass fits

$$\begin{aligned} m_g^a &= 0.98 + 4.10 \text{ ma}, \\ m_{A_1}^a &= 1.61 + 3.30 \text{ ma}, \\ m_c^a &= 0.88 + 5.70 \text{ ma}, \\ m_N^a &= 1.21 + 9.00 \text{ ma}, \end{aligned} \quad (13)$$

which correspond to the solid lines in Fig. 2b. It should be noted that the dependence of the hadron masses (13) on the quark mass is rather weak.

To compare with experiment we shall use the same (universal) $\Lambda_{\text{nom}} = 200 \text{ MeV}$ as before, which results in the lattice spacing (2). We then find that m_π takes its experimental value for $ma \approx 0.005$ (cf. Fig. 2a), which corresponds to an invariant quark mass, (10), of

$$m_q \approx 7 \text{ MeV}. \quad (14)$$

To evaluate the g , A_1 , c and nucleon masses at the (physical) quark mass (14) we shall use the linear mass formulae (13). In physical units we then obtain (including statistical errors; cf. Fig. 2b)

$$\begin{aligned} m_g &= (730 \pm 90) \text{ MeV}, \\ m_{A_1} &= (1190 \pm 90) \text{ MeV}, \\ m_c &= (660 \pm 50) \text{ MeV}, \\ m_N &= (920 \pm 100) \text{ MeV}. \end{aligned} \quad (15)$$

We notice that $\Lambda_{\text{nom}} = 200 \text{ MeV}$ fits the low-lying hadron masses quite well (given the statistical errors). From the slope of $(m_a)^2$ versus ma , (12), and using the calculated value of $\langle \bar{\psi}\psi \rangle^{1/3}$ (i.e. $\langle \bar{\psi}\psi \rangle^{1/3} = (235 \pm 10) \text{ MeV}$), we also extract

$$f_\pi \approx 134 \text{ MeV}. \quad (16)$$

This is to be compared to the experimental value of (19) $f_\pi = (131.9 \pm 0.1) \text{ MeV}$.

The c meson will mix with the O^{++} glueball, which we have not taken into account. It is interesting to note that both masses, m_c and $m(O^{++})$, are close (11) ($m(O^{++}) = (740 \pm 40) \text{ MeV}$).

We may say that we obtain altogether a consistent picture of quark and gluon physics in quenched QCD (in contrast to Monte Carlo calculations using Wilson fermions). We are in the process of redoing the calculation at different β values to check for continuum renormalization group behaviour. We are also calculating the masses of various other states.

Encouraged by the success of the calculations so far we are currently analyzing whether the explicitly broken $SU(4)$ chiral symmetries are dynamically restored in the region of β where we can perform calculations, and if these symmetries are restored, whether they are spontaneously broken with correspond-

ing Goldstone "pions". We have learned that similar questions, in the context of colour SU(2), are also being addressed by the Saclay group (20).

The numerical calculations have been done on the Siemens 7.882 at the University of Hamburg and on the Cyber 205 at the University of Karlsruhe. The estimated average speed of our matrix inversion program on the Cyber 205 is \approx 60 Mega-flops. Due to the sparsity of the matrix almost half the time is spent to "gather" the desired matrix elements and store them consecutively. To fit the program into the available main memory of \approx 7 Megabytes some tricks were necessary, which slowed the program down further.

Acknowledgement

We are grateful for the support of the DESY directorate in purchasing time on the Cyber 205 and for the generous facilities provided by the University of Hamburg. We are indebted to Drs. D. Ponting and Ian Duff for useful discussions and to Dr. Schäfer from CDC for computational assistance. M.T. thanks Dr. Tom Walsh and Prof. F. Gutbrod for the hospitality of the DESY Theory Group during part of this work, and J.P.G. thanks the SERC and the Royal Society for a fellowship.

References

- 1) J. Kogut, L. Susskind: Phys. Rev. D11, 395 (1975);
L. Susskind: Phys. Rev. D16, 3031 (1977);
I. Banks, J. Kogut, L. Susskind: Phys. Rev. D13, 1063 (1976);
I. Banks, S. Raby, L. Susskind, J. Kogut, D.R.T. Jones, P.N. Scharbach,
D. Sinclair: Phys. Rev. D15, 1111 (1976);
H.S. Sharatchandra, H.J. Thun, P. Weisz: Nucl. Phys. B192, 205 (1981).
- 2) K.G. Wilson: Erice lectures (1975).
- 3) H. Hamber, G. Parisi: Phys. Rev. Lett. 47, 1792 (1981);
E. Marinari, G. Parisi, C. Rebbi: Phys. Rev. Lett. 47, 1795 (1981);
D. Weingarten: Phys. Lett. 109B, 57 (1982);
A. Hasenfratz, P. Hasenfratz, Z. Kunszt, C.B. Lang:
Phys. Lett. 110B, 289 (1982).
- 4) D. Weingarten: Nucl. Phys. B215, 1 (1983);
F. Fucito, G. Martinelli, C. Omero, G. Parisi, R. Petronzio, F. Rapuano:
Nucl. Phys. B210, 407 (1982);
R. Gupta, A. Patel: preprint CALT-68-966 (1982);
A. Hasenfratz, P. Hasenfratz, Z. Kunszt, C.B. Lang:
Phys. Lett. 117B, 81 (1982).
- 5) P. Hasenfratz, I. Montvay: Phys. Rev. Lett. 50, 309 (1983);
G. Martinelli, G. Parisi, R. Petronzio, F. Rapuano:
Phys. Lett. 122B, 283 (1983);
R. Gupta, A. Patel: Phys. Lett. 124B, 94 (1983);
C. Bernard, T. Draper, K. Olynyk: Phys. Rev. D27, 227 (1983)
- 6) H. Lipps, G. Martinelli, R. Petronzio, F. Rapuano:
CERN preprint TH-3548 (1983)
- 7) P. Hasenfratz, I. Montvay: DESY preprint 83-072 (1983)
- 8) M. Fukugita, T. Kaneko, A. Ukawa: Tokyo preprint INS-Rep.-472 (1983)

9) I.M. Barbour, J.P. Gilchrist, G. Schierholz, H. Schneider, M. Teper: Phys. Lett. 127B, 433 (1983)

10) For a general discussion see e.g.:
F. Szidarovszky, S. Yakowitz: Principles and Procedures of Numerical Analysis. (Plenum Press, 1976);
D. Luenberger: Introduction to Linear and Non-Linear Programming (Addison-Wesley, 1973);
L. Hagemann, D. Young: Applied Iterative Methods (Academic Press, 1981);
A. Ralston, H. Wilf: Mathematical Methods for Digital Computers (Wiley, 1960);
For modern techniques and applications see e.g.:
I.S. Duff: A Survey of Sparse Matrix Software, Harwell preprint AERE-R 10512 (1982);
I.S. Duff, G.S. Stewart (Eds.): Sparse Matrix Proceedings 1978 (SIAM Press, 1979);
I.S. Duff (Ed.) Sparse Matrices and their Uses (Academic Press, 1981);
J. Bunch, D. Rose (Eds.): Sparse Matrix Computations (Academic Press, 1976).

11) K. Ishikawa, A. Sato, G. Schierholz, M. Teper: DESY preprint 83-061 (1983), to be published in Zeitschr. f. Physik C.

12) M. Teper: talk at the International Europhysics Conference on High Energy Physics, Brighton (July 1983);
G. Schierholz, M. Teper: in preparation.

13) I.M. Barbour, P. Gibbs, J.P. Gilchrist, G. Schierholz, H. Schneider, M. Teper: DESY preprint 83-093 (1983).

14) F. Gutbrod, P. Hasenfratz, I. Montvay, Z. Kunszt: CERN preprint TH-3591 (1983).

15) K.G. Wilson: Phys. Rev. D10, 2445 (1974).

16) N. Kawamoto, J. Smit: Nucl. Phys. B192, 100 (1981).

17) H. Kluberger-Stern, A. Morel, O. Napoly, B. Petersson: Saclay preprint DPh/83/29 (1983);
J. Kogut, M. Stone, H. Wylid, S. Shenker, J. Shigemitsu, D. Sinclair: Illinois preprint DOE/ER/01545-335 (1983).

18) H. Hamber, G. Parisi: Phys. Rev. D27, 208 (1983).

19) J. Gasser, H. Leutwyler: Phys. Reports 87C, 78 (1982).

20) A. Billoire, R. Lacaze, E. Marinari, A. Morel, P. Windey: private communication.

Figure Captions

Fig. 1 $\langle \bar{\psi}\psi \rangle$ as a function of the bare (renormalization group invariant) quark mass $ma(m_q)$ obtained on the $4^3 \cdot 8$, $6^3 \cdot 8$ and 8^4 lattice at $\beta = 5.7$ using the Lanczos algorithm. The solid circles come from the hadron spectrum calculation on the $10^3 \cdot 16$ lattice in this paper, using the conjugate gradient algorithm, and are obtained from a total of 112 rows ($\times 3$ colours) of the inverse of the fermion matrix.

Fig. 2a $(m_q a)^2$ as a function of $ma(m_q)$. The solid circle on the linear extrapolation curve marks the position of the physical pion, using (1), (2) as our scale, from which we can read off the value of m_q .

Fig. 2b The hadron masses, $m_H a$, as a function of $ma(m_q)$. The solid circles at the physical quark mass indicate their experimental values using (1), (2).

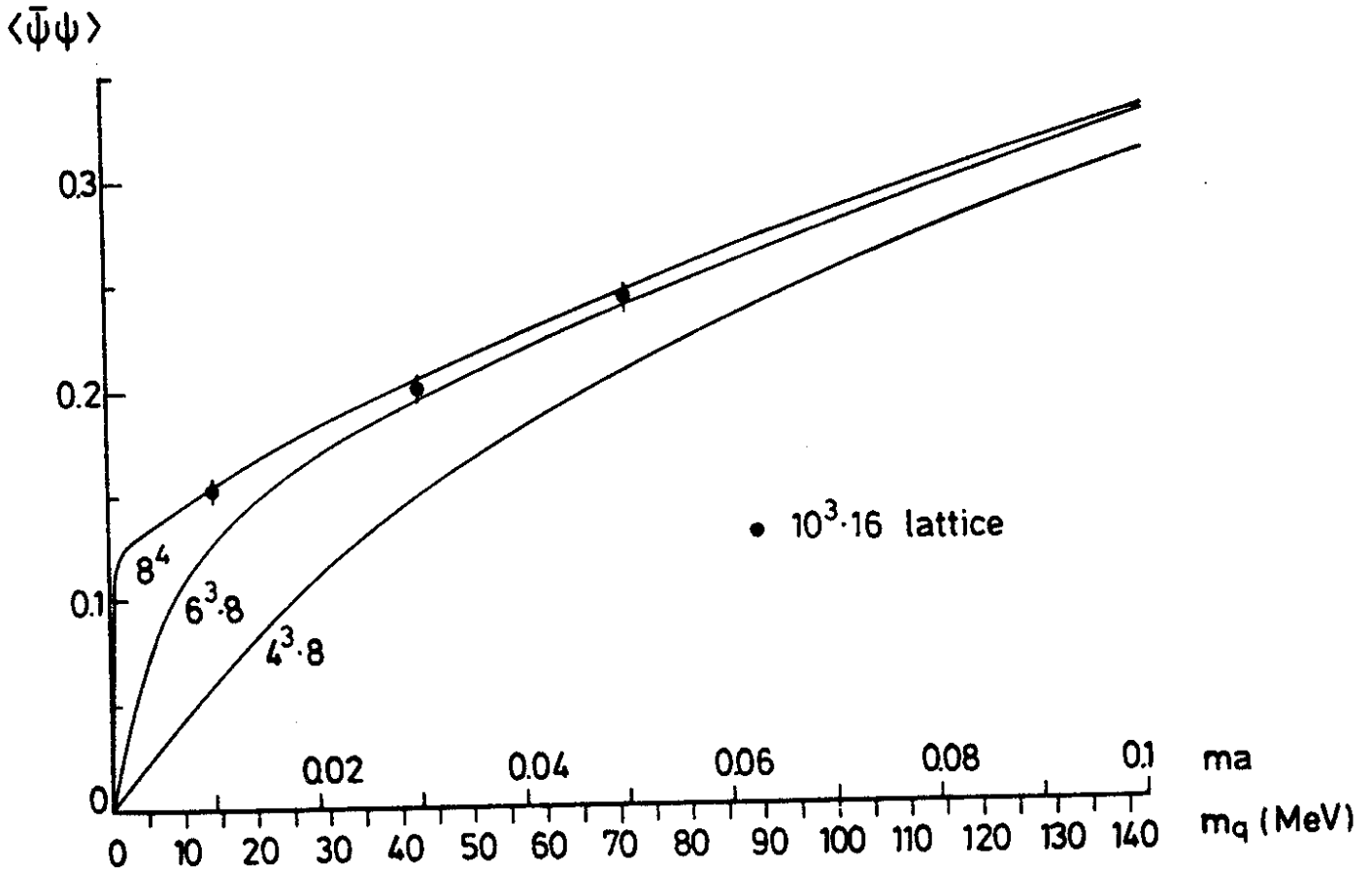


Fig.1

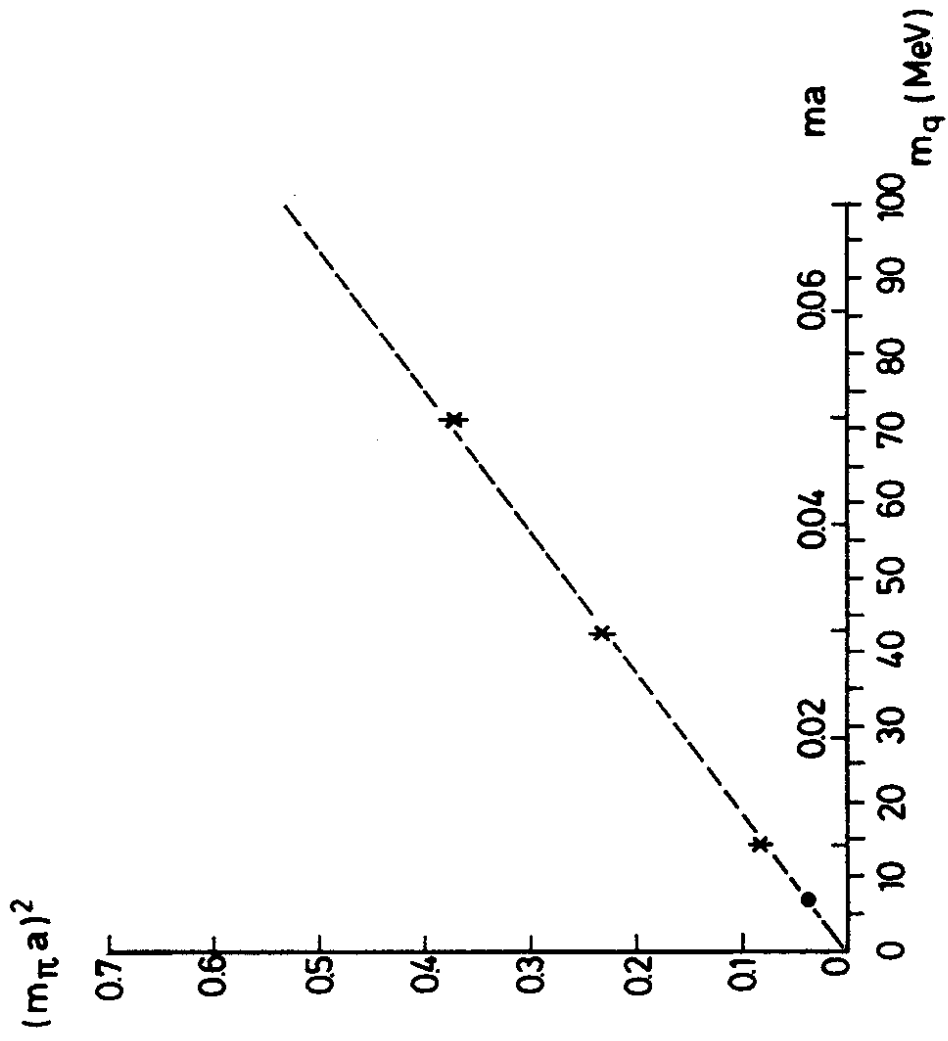


Fig.2a

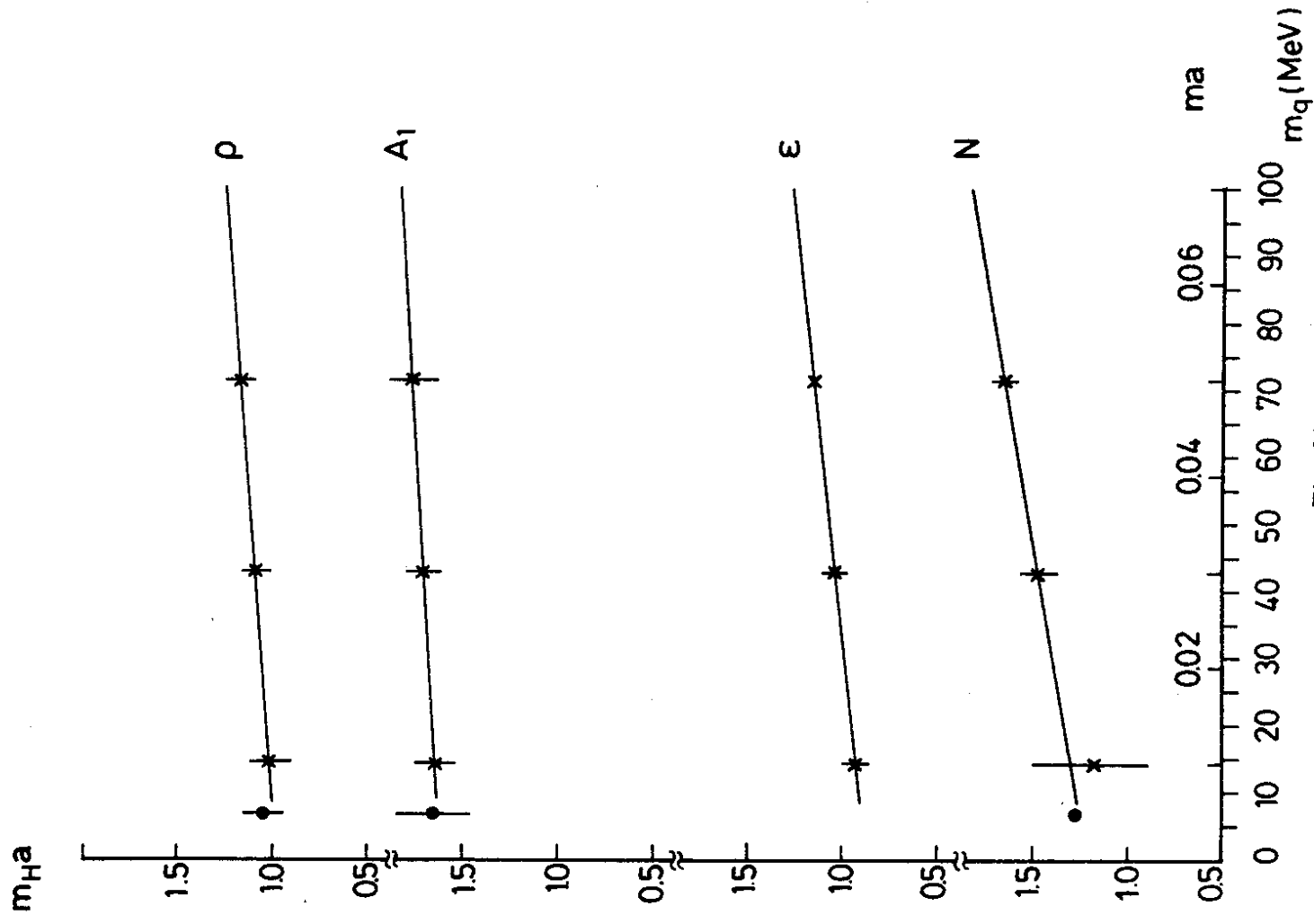


Fig.2b

